J. Sound Vib. (1970) **13** (4), 389–408

THE RADIATION OF SOUND FROM AN ENGINE EXHAUST

R. J. ALFREDSON† AND P. O. A. L. DAVIES

Institute of Sound and Vibration Research, University of Southampton, Southampton, SO9 5NH, England

(*Received* 21 *October* 1969, *and in revised form* 9 *February* 1970)

This paper reports the findings of the first stage of a systematic investigation of the processes occurring in an internal combustion engine exhaust system. It deals initially with finite amplitude pressure wave effects. The boundary conditions imposed on the fluctuating pressure in the exhaust system by the exhaust outlet are then discussed on the basis of measurements made using the tail pipe as an impedance tube. The nett energy flux in the tail pipe including the effect of mean flow is calculated and subsequently related to the level of the sound radiated by the engine exhaust.

1. INTRODUCTION

Acoustic theory has been widely used for designing exhaust silencers for internal combustion engines. This theory is based on replacing exhaust ports (valves) by a single source of acoustic signals while considering that the exhaust system behaves as an idealized acoustic transmission line. The silencers thus evolved, [1–9] for example, have usually reduced the noise emitted by the exhaust, but this limited success does not really justify uncritical acceptance of the method.

The performance achieved by the silencers has often been inferior to that expected. This has been widely attributed to the presence of finite amplitude waves which invalidate the linearization assumptions of the acoustic theory. It is therefore important first to determine the magnitude of the pressure fluctuations in typically noisy exhaust systems and to consider then whether these are sufficiently large to cause significant deviations from the linearized theory.

Regardless of whether finite amplitude effects are important or not, one should, in seeking reasons for the discrepancy between the predicted and achieved performance, examine at least four other features of the traditional approach, namely: (i) neglect of mean gas flow and, in particular, its effect on nett energy transport; (ii) simplified boundary conditions for the exhaust ports and exhaust outlet; (iii) neglect of interaction between mean gas flow and sound in regions of disturbed flow; (iv) neglect of mean temperature variation along the exhaust system.

It will be shown that the mean gas flow makes an important contribution to the nett energy transport in exhaust systems. Its omission, therefore, can lead to serious errors in predicted levels of sound radiated by the exhaust.

It can readily be demonstrated that the boundary conditions imposed by the exhaust outlet determine basically what proportion of the energy arriving at the exhaust outlet is radiated. The level of this energy arriving at the outlet is in turn influenced, for any given system, by the boundary conditions imposed by the exhaust ports. It is obviously important to represent realistically both these conditions for any inaccuracy here will have a significant effect on the predicted performance of an exhaust system.

† Present address: NASA Langley Research Center, Hampton, Virginia, U.S.A.

Since there were several areas of uncertainty, it was recognized that a systematic investigation based on measurements in practical exhaust systems was necessary to produce a more accurate basis for silencer design. There also seemed obvious advantages in subdividing the complete system into a source region (exhaust ports and manifold) a silencer section and a tail pipe. The present paper deals with conditions found in the exhaust tail pipe. Two further papers will deal in detail with the performance of other components of the exhaust system.

A survey of a number of representative high performance internal combustion engines showed that the general tail pipe conditions were insensitive to the engine type and so it was necessary to investigate only one in detail. This was a six-cylinder, two-stroke diesel engine which developed approximately 200 b.h.p. at a crankshaft speed of 2200 rev/min. The engine was known to have a serious exhaust noise problem.

Initially the effects of finite amplitude pressure waves in the tail pipe were considered. The boundary conditions imposed by the exhaust outlet were then investigated and as a consequence of this the nett energy transport in the tail pipe was calculated. Finally this energy was related to the level of the sound radiated at the exhaust outlet.

2. FINITE AMPLITUDE WAVES

The characteristic feature of finite amplitude pressure waves as compared with acoustic waves is that their waveforms continually change. This waveform variation can be calculated by the method of "characteristics" [10]. This process has been computerized and extensively exploited, e.g. [11, 12], for one-dimensional investigation of gas exchange processes during exhausting and for matching of turbochargers to engines. The results have been encouraging but the method remains expensive, even for simplified systems. Probably for this reason there are no known reports dealing specifically with its application to silencer designs. For a typical installation the merits of a large number of different silencer layouts have to be evaluated and the cost for this would be prohibitive at present.

The question remains whether finite amplitude effects in the tail pipe are of practical significance. Some insight can be obtained by considering an initially sinusoidal wave as shown in Figure 1. Provided the disturbance remains one-dimensional, it will transform ideally into a series of travelling normal shocks. We calculated the transformation in the waveform illustrated with a digital computer using the method of characteristics. The relation between frequency, pressure ratio and time required to shock was obtained by summarizing the results of a systematic series of calculations. It was found, for example, that sinusoidal pressure fluctuations with an amplitude of 1–2 lb/in^2 became steep in a time, T, given approximately by

$$T = \frac{p_0}{5.f.\Delta p}, \tag{1}$$

where p_0 is the mean pressure, Δp the amplitude of the pressure wave, and f the wave frequency.

The corresponding distance travelled by a sinusoidal wave before shock formation occurs is then approximately

$$\text{distance} = T.(C \pm w_0), \tag{2}$$

where C is the mean sonic velocity and w_0 is the mean velocity of the gas flow. The positive sign applies to waves travelling with the mean flow and the negative sign refers to waves travelling against the flow.

Thus a sinusoidal wave of amplitude $\pm$ 1 lb/in^2, i.e. 167·7 dB, and frequency of 300 Hz (this is typical of the frequency where maximum pressure levels occur) will shock in the presence of a mean flow of 100 ft/sec after travelling a distance of about 15 ft.

The above example is greatly simplified for, on this basis, any plane progressive wave, even a weak acoustic one, would shock after travelling a finite distance. In fact, the steepening phenomena are opposed by various irreversible dissipation processes [13] which are frequency dependent and are characteristic of the medium. The eventual steepness of the waveform or the distance travelled before shock formation will depend on these processes as well as the initial conditions of the wave. Thus the distance to shock is always greater than the above example suggests.

In an exhaust system, incident waves and waves reflected at area discontinuities are present simultaneously and consequently the calculation of a distance to shock is hardly practical since the solutions are no longer unique.

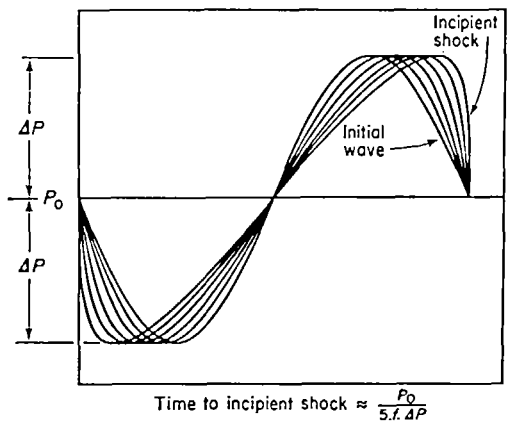

Figure 1. Variation of sinusoidal wave (neglecting dissipation). f = wave frequency.

A further complication is that energy is radiated at the exhaust outlet, which modifies the waveform further. Since the higher frequencies are radiated more efficiently, the reflected waves are less steep than the incident ones.

As a first estimate, one may assume on the basis of the above discussion that below a pressure level of, say, 160 dB at frequencies typically of the order of 300 Hz, the finite amplitude effects should be small enough to neglect.

Measurements of the sound pressure level in a number of exhaust tail pipes showed in fact that the maximum levels there were of the order of 155 dB at 300 Hz and about 135 dB at 1000 Hz. (The total radiated sound pressure level was in the region of 120 dB at a distance of 3 ft from the exhaust outlet.) Consequently, it seemed reasonable that the linearized theory would suffice for the conditions in the tail pipe and the analysis proceeded on this basis.

3. RADIATED SOUND

It may readily be demonstrated that the level of the radiated sound is a function of the exhaust system, the engine speed and load. Some appreciation of the effects of load and speed can be seen in Figure 2. These results were obtained by recording the sound pressure level at a distance of 3 ft from the outlet of the standard exhaust system while the engine speed was slowly changed between the two extremes. The engine was contained within a sound-proofed test room and the exhaust pipe protruded out through a side wall terminating about 10 ft from the wall and 6 ft above the ground and radiating into relatively free space.

As noted in [15] and [16], the A-weighting gives an approximate measure of the "loudness" of the exhaust. It is seen that increasing the speed causes an increase in loudness both at no

load and full load. The overall sound pressure level similarly increases although at full load there are some louder resonances at speeds of 1150 and 1650 rev/min. This behaviour is typical of reactive-type silencers but is not easily predicted since one has to consider the resonances of the entire exhaust system which are often not simply related to resonances of individual components.

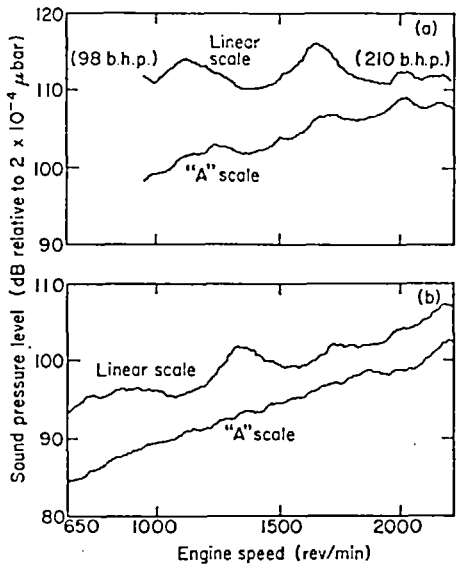

Figure 2. Variation of exhaust noise with speed. (a) With full load, (b) with no load.

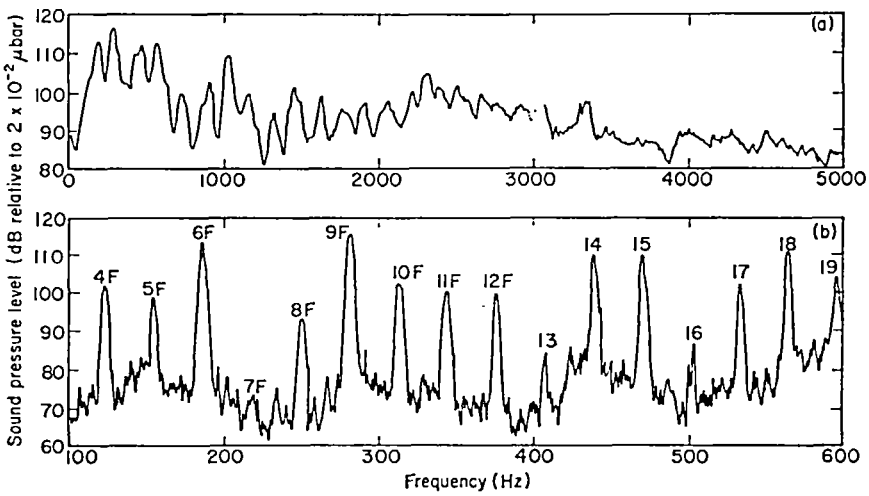

Figure 3. Typical spectrum of exhaust noise (a) 3 ft from outlet; 50 Hz filter, (b) 3 ft from outlet; 3 Hz filter. Crankshaft speed, 1880 rev/min; fundamental, 31·4 Hz.

A typical spectrum of the exhaust noise, where the silencer was a simple expansion chamber, for a crankshaft speed of 1880 rev/min is given in Figure 3. The spectrum extends from very low frequencies up to a few kHz, with the largest amplitudes occurring in the region of 100–1000 Hz. Measurements of a number of other systems confirm that this behaviour is typical.

The narrow-band analysis of a section of the spectrum shows, not surprisingly (since a purely sinusoidal excitation would not be expected), that the exhaust noise consists of a

large number of discrete frequency components. These are all harmonics of the firing frequency, i.e. crankshaft speed (rev/sec). These discrete frequency components were found up into the kHz region of the spectrum and showed that the contribution from the broad-band jet noise of the gas flow was insignificant.

Since the highest amplitudes occurred in the lower frequency range, most attention has been concentrated on these components. Wavelengths are thus very large compared with the pipe radius. Consequently one could reasonably expect that only the plane mode (i.e. the

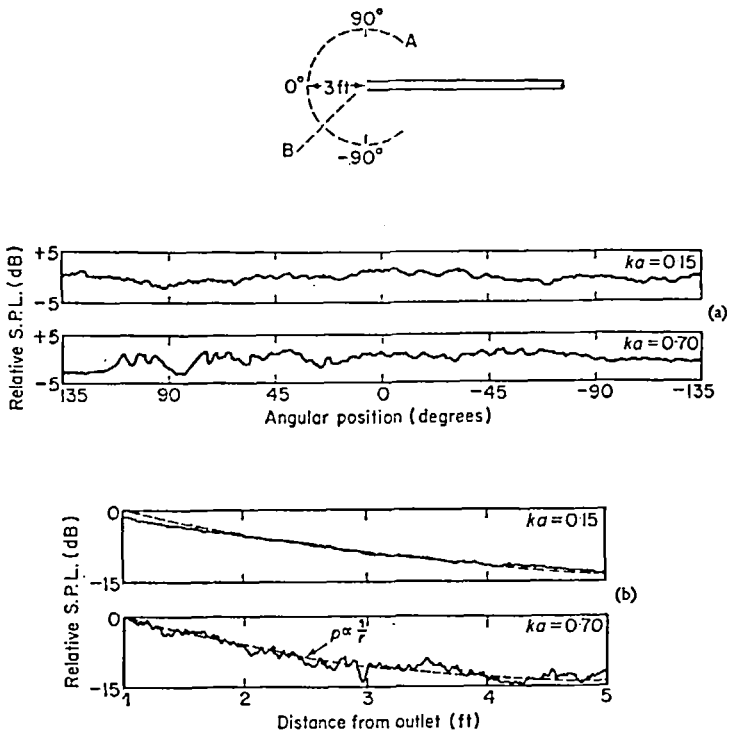

Figure 4. Radiated sound characteristics. (a) Directivity patterns along path "A". (b) Sound pressure level—distance relation along path "B".

0,0 mode using the terminology of [17]) will propagate along the pipe [17]. Further, since the pipe radius is small compared with the wavelengths, the exhaust outlet was considered as a source of approximately spherically diverging waves.

To establish this latter feature, measurements were made of the sound pressure level, typical results being as shown in Figure 4. The lack of directivity and the inverse pressure–distance relationship indicate that in practical terms free-field conditions exist and that the sound is spherically diverging. Consequently measurements of the radiated sound pressure were made at a distance of 3 ft from the exhaust outlet and calculation of energy flux assumed spherically diverging waves.

4. BOUNDARY CONDITIONS IMPOSED BY EXHAUST OUTLET

Basically, one is interested in the behaviour of the incident sound from the engine arriving at the exhaust outlet. Generally, it would be expected that partial transmission and partial reflection would occur there with the reflected wave shifted in phase and reduced in amplitude relative to the incident one. This information is fundamental in exhaust system designs since

it sets a boundary condition for the pressure fluctuations in the exhaust pipe and allows also the calculation of the level of the radiated sound from pressure measurements in the tail pipe.

Four different assumptions have been applied in the past to describe this reflection and transmission process, namely, (i) reflection coefficient zero, e.g. [2]; (ii) reflection coefficient unity, phase angle zero, e.g. [2, 4]; (iii) reflection coefficient and phase angle given by the zero mean flow acoustic theory [14], e.g. [1]; (iv) infinite transmission line, e.g. [5].

Condition (i) implies that there are no standing waves in the tail pipe, that all the sound is radiated and that the performance of the exhaust system is not affected by the length of the tail pipe. Measurements made in several exhaust tail pipes show that these assumptions are all violated and it seems, therefore, that a reflection coefficient of zero is grossly in error for exhaust systems.

Condition (ii) (which, incidentally, is that used in the method of characteristics) allows standing waves to develop in the tail pipe and consequently the performance of the silencer is affected by the tail pipe length. It ignores, however, the variation with frequency of the radiation efficiency and thus produces large errors in calculating radiated sound pressure levels particularly at higher frequencies. Thus this assumption, while better than (i), is still in error.

Condition (iii) overcomes the objections raised above but its application to an exhaust system is still doubtful. The presence of the mean gas flow and the large difference in temperature between this and that of the air surrounding the pipe could be expected to alter reflection and transmission phenomena. Measurements have been made [18] of the reflection coefficient and phase angle (in the presence of a steady mean flow at ambient conditions) at the exit of a flanged circular pipe using a loudspeaker as the source of signals. This showed that the phase angle was relatively insensitive to mean flow but that the reflection coefficient increased by a factor of $1 + 2M$ where M is the Mach number of the flow. At very low frequencies, the increase was less. These results cannot be applied directly to the exhaust system because the conditions there, elevated gas temperatures and possibly pulsating gas flow, are significantly different to those above. They do suggest, however, that assumption (iii) may not be accurate for exhaust systems.

The fourth assumption, namely, that the exhaust tail pipe is part of an infinite transmission line, is obviously in error since the exhaust system is definitely finite. This approach perhaps may be of some value but it cannot be recommended.

Clearly the measurement of the reflection coefficient and phase angle in an exhaust pipe, using the engine exhaust as the source of signals, would resolve the boundary conditions at the exhaust outlet and would remove one of the sources of error persistently occurring in exhaust system analysis. The conditions, experimentally, are difficult, but it was considered worthwhile to attempt this since the results would be directly applicable to the exhaust system. An alternative would have been to measure the reflection coefficient and phase angle in a pipe with a heated mean flow and a loudspeaker as source. The experimental conditions there would be more ideal but there would always be uncertainty when those results are applied to a different situation, namely the exhaust pipe.

5. IMPEDANCE TUBE THEORY APPLIED TO AN EXHAUST PIPE

A number of methods exist for measuring the reflection coefficient and phase angle in the absence of mean flow, as, for example, summarized in [19]. The method most commonly used for normal incidence is that based on the impedance tube [20]. The technique is so well established that there is little need to discuss it in any detail. Basically, the reflection coefficient is obtained from the standing wave ratio and the phase angle from the distance of the first minimum from the outlet compared with the distance between subsequent minima.

This method seemed the most suitable for the tail pipe investigation but before it can be applied, the influence of gas flow needs consideration.

It is well established that the fluctuating pressure, p', for axially symmetric waves in a cylindrical tube in the presence of mean flow, shear, viscosity and yielding tube walls can be represented by

$$p' = A.P_1(r).e^{i[\omega t-(k_1+ik_2)z]} + B.P_2(r).e^{i[\omega t-(k_3+ik_4)z]}, \tag{3}$$

where $P_1(r)$ is the radial variation in pressure of the positive-going wave, $P_2(r)$ the radial variation in pressure of the negative-going wave, A,B the amplitude of the positive- and negative-going waves, respectively, k_1,k_2 the real and imaginary parts of wave number of A, k_3,k_4 the real and imaginary parts of wave number of B, ω the angular frequency, and z the distance in the axial direction.

[It is understood that physical significance is attributed only to the real part of (3) and subsequent similar equations. The sign convention used for the wave numbers, namely, $-(k_1 + ik_2)$ and $-(k_3 + ik_4)$, was chosen basically for convenience in the solution of subsequent equations on a digital computer. It is convenient also that the real part of the wave number is positive for a positive-going wave and negative for a negative-going wave.]

Providing the variation in pressure with radius is small (and this will be shown to be the case for the present analysis, section 7) the above equation can be replaced by

$$p' = A_1.e^{i[\omega t-(k_1+ik_2)z]} + B_1.e^{i[\omega t-(k_3+ik_4)z]}, \tag{4}$$

where

$$\frac{B_1}{A_1} = R.e^{i\theta}, \qquad \text{i.e. } B_1 = R.A_1.e^{i\theta}, \tag{5}$$

R is the reflection coefficient at the exhaust outlet, i.e. $z = 0$, θ the phase angle between the reflected wave and the incident wave at $z = 0$, and A_1,B_1 the amplitude of the positive- and negative-going waves, respectively.

Although it is not obvious at this stage, it is possible, with a mean gas flow, for the reflection coefficient, R, slightly to exceed unity without reversal in energy flux (section 7). Under these circumstances, it appears that, from consideration of pressure fluctuations alone, the source and receiver of sound in the pipe have been reversed [21]. It is then more convenient to express the pressure fluctuations by

$$p' = A_2.e^{i[\omega t-(k_1+ik_2)z]} + B_2.e^{i[\omega t-(k_3+ik_4)z]}, \tag{6}$$

where

$$\frac{B_2}{A_2} = R.e^{i\theta}; \qquad \text{i.e. } A_2 = \frac{B_2}{R}.e^{-i\theta} \tag{7}$$

and R and θ are as defined above.

As a result of interference between incident and reflected waves, standing wave patterns will develop whose amplitudes can be shown simply from (4) and (6), respectively, to be

$$|p'| = A_1\{e^{2k_2z} + R^2.e^{2k_4z} + 2Re^{(k_2+k_4)z}\cos[\theta + (k_1 - k_3)z]\}^{1/2} \tag{8}$$

for $R < 1{\cdot}0$,

$$|p'| = B_2\left\{\frac{e^{2k_2z}}{R^2} + e^{2k_4z} + \frac{2}{R}e^{(k_2+k_4)z}\cos[\theta + (k_1 - k_3)z]\right\}^{1/2} \tag{9}$$

for $R > 1{\cdot}0$. [Both A_1 and B_2 can be chosen as real quantities in (4) and (6), respectively.]

Equations (8) and (9) have maxima and minima when the cosine term has a value of $+1{\cdot}0$ and $-1{\cdot}0$, respectively. The ratio of these maxima to minima, i.e. the standing wave ratio, is given by

$$\text{ratio} = \frac{1 + R.e^{(k_4-k_2)z}}{1 - R.e^{(k_4-k_2)z}} \tag{10}$$

for $R.e^{(k_4-k_2)z} < 1{\cdot}0$, and

$$\text{ratio} = \frac{1 + R.e^{(k_4-k_2)z}}{R.e^{(k_4-k_2)z} - 1{\cdot}0} \tag{11}$$

for $R.e^{(k_4-k_2)z} > 1{\cdot}0$. These equations differ slightly from that given in [21], namely,

$$\text{ratio} = \frac{1 + R.e^{2\alpha z}}{1 - R.e^{2\alpha z}}, \tag{12}$$

where $\alpha = \alpha_0/(1 - M^2)$, and α_0 is the imaginary part of the wave number in the absence of mean flow.

It is noted that the ratio in (12) becomes negative when $R.e^{2\alpha z} > 1{\cdot}0$. Further, one finds that, in general, with shear and yielding walls,

$$k_4 - k_2 \neq 2\alpha_0/(1 - M^2).$$

In the absence of a mean flow, however, the relationship is valid, namely,

$$k_4 - k_2 = 2\alpha_0.$$

Whether R is greater than or less than unity can usually be resolved by observing the standing waves. If R is greater than unity, the ratio given in (11) increases as z moves from the exhaust outlet towards the engine. If R is less than unity, the ratio given in (10) decreases monotonically. Alternatively, one may compare the phase of the signal with a reference signal as z moves towards the engine [21]. For R greater than unity, one is apparently moving away from the "source" while with R less than unity one is moving towards the source.

At the exhaust outlet, i.e. at $z = 0$, the ratios given in (10) and (11) become

$$\text{ratio} = \frac{1 + R}{R - 1} \tag{13}$$

for $R > 1{\cdot}0$, and

$$\text{ratio} = \frac{1 + R}{1 - R}, \tag{14}$$

for $R < 1{\cdot}0$, which allows the value of the reflection coefficient to be evaluated. Thus, if the line joining the maxima and the line joining the minima are both projected to the outlet, the standing wave ratio (on a decibel scale) can be read and the reflection coefficient follows immediately. The latter procedure is precisely that used in the absence of mean flow.

The positions of the minima occur, as noted previously, when the cosine term in equations (8) and (9) is equal to $-1{\cdot}0$, i.e.

$$\cos[\theta + (k_1 - k_3)z] = -1{\cdot}0 = \cos(-\pi, -3\pi, -5\pi, \text{etc.}).$$

Thus the ratio, n, of the distance from the outlet to the first minimum, to that of the distance between the subsequent minima is given as

$$n = (\theta + \pi)/2\pi. \tag{12}$$

This is again identical to that of the zero flow case and therefore allows the phase angle to be computed. Note that the distance between the minima (or maxima) namely $2\pi/(k_1 - k_3)$ is no longer equal to a half wavelength as would be the case for zero flow in the absence of any losses. This, in effect, can be considered as a change in length of the impedance tube although the "increase" is quite small for the Mach numbers typically found in exhaust systems.

From the above it is seen that while mean flow, shear, viscosity and yielding walls all alter the standing wave pattern, the basic information concerning reflection coefficient and phase angle at the exhaust outlet can still be extracted. Note that the method of excitation of the

signals does not affect these conclusions. It is thus now possible to proceed to use the exhaust tail pipe as an impedance tube to measure reflection coefficients and phase angles.

6. MEASUREMENT OF SOUND PRESSURE LEVEL IN THE EXHAUST TAIL PIPE

A continuously traversing pressure transducer was constructed so that the sound pressure in the exhaust system could be measured over a distance of 5 ft 6 in. An electric motor driving a screw thread provided the motion—forward and reverse—and a piezo-electric pressure transducer mounted in a steel tube (Figure 5) supplied the signal which was amplified and recorded on a Nagra tape recorder.

Temperatures in the exhaust system varied considerably with load and speed and were typically in the region of 100°C to 350°C at the exhaust tail pipe. Cooling was provided by circulating water for the pressure transducer and compressed air for the cable connecting the pressure transducer to the charge amplifier.

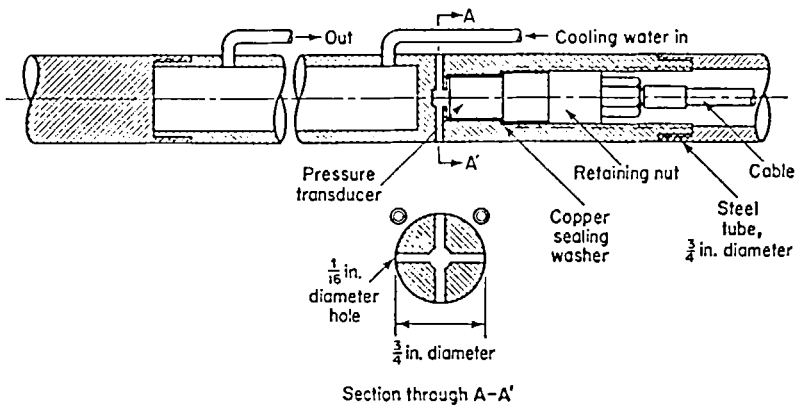

Figure 5. Pressure transducer mounting.

To avoid the effect of changing the cross-sectional area of the exhaust pipe as the pressure transducer traversed, the steel tube in which the pressure transducer was mounted was extended forward a distance of 6 ft 6 in. into a simple expansion chamber (12 in. diameter, 6 ft long) connected to the exhaust manifold. The tube area was then about ¼% that of the expansion chamber area.

The signal-to-noise ratio of the entire set-up was better than 50 dB.

Gas velocity profiles were measured with a pitot tube and it was found that the mean value was about 85% that of the midstream value. Because the gas flow would be pulsating to some extent there must be uncertainty concerning the accuracy of these measurements. Nevertheless, the calculated mass flow rates in the exhaust system correspond very closely to the values provided by the engine manufacturer.

Tests were conducted at constant engine speed and load. Generally the inevitable fluctuations in both these quantities due to imperfect governing were not large enough to present serious problems except in the region of maximum speed and load. In this region, the cooling of the pressure transducer was barely adequate. Consequently full power tests were not conducted but as the overall sound pressure level was higher at lower speeds (Figure 2) this was not considered an important limitation. The fact that the engine speed was varying slightly can be seen by the ripple on the standing waves in Figures 6 and 7.

The pressure fluctuations in the tail pipe of a number of exhaust systems were recorded commencing at the outlet and traversing towards the engine. The average indicated sound

pressure level at a distance of 3 ft from the exhaust outlet was measured following the recommended procedure [22].

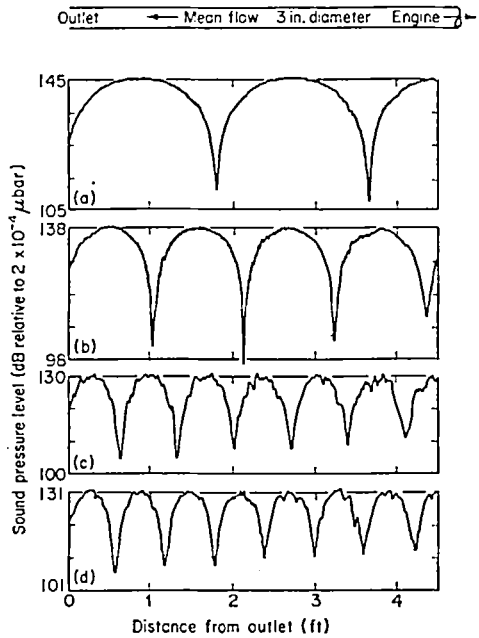

Figure 6. Typical standing waves at mean flow of 0·078 *M*. (a) 228 Hz, (b) 342 Hz, (c) 685 Hz, (d) 980 Hz.

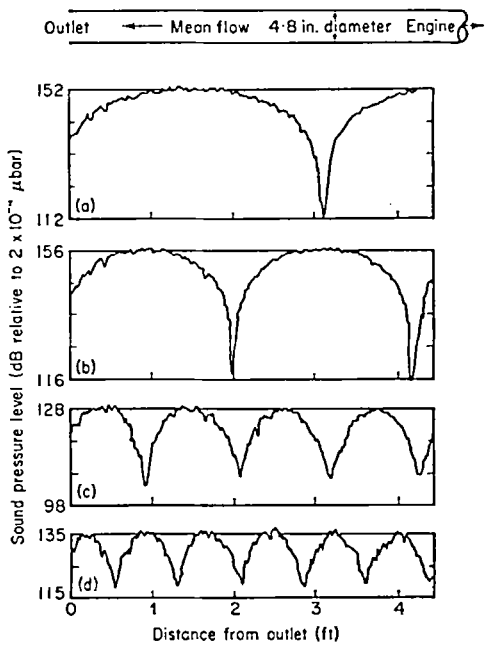

Figure 7. Typical standing waves at mean flow of 0·171 *M*. (a) 385 Hz, (b) 610 Hz, (c) 965 Hz, (d) 1105 Hz.

As noted previously, the level of the pressure fluctuations were small compared with the mean value. Consequently, each frequency component in the total signal could be investigated individually since the principle of superposition allows the decomposition of the total signal into its component signals.

The standing wave patterns for each component were extracted from the total signal using a 10 Hz constant bandwidth filter tuned in turn to the various frequencies. An investigation of the various filter types had shown that this particular filter was the best compromise. The problem basically is one of measuring the minima of the standing waves. The separation between the components is obviously a function of engine speed but is typically of the order of 25–35 Hz, e.g. Figure 2. Since filters do not have sharp cut-offs, there is the danger that, at a minimum, overlap from the adjacent discrete components will result in an overestimation of the minimum. However, the situation is not quite as severe as might appear at first sight. When the signal from the component under consideration is passing through a minimum, the two adjacent components will be close to their respective minimums and will therefore be similarly small in amplitude. Standing wave ratios of the order of 40 dB could be measured consistently. Ratios greater than 45–50 dB were suspect because of filter overlap.

Obviously, the use of a narrower filter, e.g. 3 Hz, would enable greater standing wave ratios to be measured. One now encounters more serious engine speed variation problems and consequent occasional loss of signal particularly at higher frequencies. This produces erratic standing wave curves.

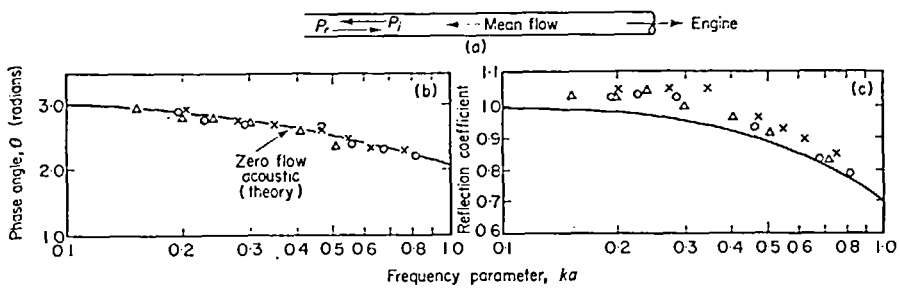

Figure 8. Reflection of sound. (a) Exhaust tail pipe, $P_r = R.P_i e^{i\theta}$. (b) Phase angle vs. frequency parameter. (c) Reflection coefficient vs. reflection parameter. ——, Theoretical zero flow acoustic; ○, $M = 0{\cdot}078$; △, $M = 0{\cdot}11$; ×, $M = 0{\cdot}17$.

Typical standing waves for a 3 in. and a 4·8 in. diameter pipe are shown in Figures 6 and 7. The standing wave ratio could be measured with an accuracy of about ± 2 dB. This produces an error of about ± 0·5% in the value of the reflection coefficient, R, when $R = 1{\cdot}0$, and an error of ± 5% when $R = 0{\cdot}8$. The position of the first minimum and the distance between subsequent minima could be measured to approximately $\frac{3}{32}$ in. This in turn results in an error of the order of ± 0·5% in the value of the phase angle, θ, when $\theta = 3{\cdot}0$ radians and ± 2% when $\theta = 2{\cdot}0$ radians.

The values of the reflection coefficient and phase angle for a number of typical tests are given in Figure 8 and compared with the predicted zero flow values [14]. The phase angle is reasonably close to that predicted for the zero flow case and is thus not greatly affected by the mean flow. The reflection coefficient shows the trend which might have been expected on the basis of the measurements made with cold flow in a pipe [18], namely, increasing values with increasing Mach numbers. The increase is somewhat less than the suggested factor of $1 + 2M$. This may possibly be the result of the elevated temperatures of the exhaust gases. If, for example, the flow were cooled (with the engine running at constant speed), so that the temperature of the exhaust gases was the same as that of the surroundings, the Mach number would decrease, since the mass flow is constant, thus reducing the value of the factor $1 + 2M$. At the same time, the frequency parameter, ka, would increase effectively causing the measured values to separate further from the zero flow case. It may be that the reflection coefficient

would change during this cooling process and so it is not possible to compare the present results quantitatively with those of [18].

The increase in reflection coefficient over the zero flow case is not particularly great for normal Mach numbers. It is apparent, therefore, that the exhaust outlet boundary conditions listed as (iii) in section 4 are the most appropriate of those given. These do, however, lead to a slight underestimation of the reflection coefficient. Since, as will be shown shortly, the radiated sound pressure level of the exhaust is a function of the square of the reflection coefficient, the use of boundary condition (iii) will produce errors somewhat larger than would appear at first sight.

Having established, therefore, within the experimental accuracy, the correct boundary conditions with mean flow, it is now possible to proceed to calculate the nett energy flux with some confidence.

7. ACOUSTIC ENERGY TRANSPORT IN EXHAUST TAIL PIPE

The calculation of the level of sound radiated from the exhaust tail pipe requires a knowledge of the nett acoustic energy flux in the exhaust tail pipe. This quantity, I, is given when there is a mean flow, w_0, in one direction only by [23]

$$I = \langle p' w' \rangle + \frac{M}{\rho_0 c} \langle p'^2 \rangle + M^2 \langle p' w' \rangle + \rho_0 c M \langle w'^2 \rangle, \tag{15}$$

where the brackets imply time, averaging and pressure, axial particle velocity and density have been split into mean and fluctuating components, namely,

$p = p_0 + p'$ (pressure),
$w = w_0 + w'$ (axial velocity),
$\rho = \rho_0 + \rho'$ (density),
$M = w_0/c$ Mach. no of the mean flow.

[Radial variation in fluctuating pressure and particle velocity can of course be accommodated in (15)].

The nett power is obtained by integrating equation (15) over a cross-section.

In an exhaust system where shear, viscosity and yielding of the walls of the exhaust pipe all occur simultaneously, the particle velocity (both mean and fluctuating) and the pressure all vary with radius even for the 0,0 mode. Consequently, a knowledge of this variation is required before the integration can be performed,

While it is possible to measure the variation in Mach number across the radius, the measurement of fluctuating pressure at different radial points is more difficult and that of measuring fluctuating particle velocity and the phase angle between this and the fluctuating pressure is a problem of considerable magnitude. The approach adopted here has thus been to solve the equations of continuity, momentum and energy governing the propagation of sound in a circular pipe, in the presence of mean flow, shear and viscosity. This too is rather involved when all effects are considered simultaneously but an appreciation of the magnitude of the radial variation in fluctuating pressure and particle velocity can be obtained from the following simpler situations, namely: (a) mean flow with shear, rigid and yielding walls; (b) mean flow, zero shear, rigid and yielding walls; (c) mean flow with viscosity, rigid walls.

7.1. CASE (a) MEAN FLOW WITH SHEAR, YIELDING WALLS, INVISCID

The equations of continuity, momentum and energy in cylindrical coordinates become, for axially symmetric waves, [24]

$$\frac{\partial p}{\partial t}+\frac{1}{r}\frac{\partial}{\partial r}(\rho u r)+\frac{\partial}{\partial z}(\rho w) \quad =0, \tag{16}$$

$$\rho\left\{\frac{\partial u}{\partial t}+\frac{u\,\partial u}{\partial r}+\frac{w\,\partial u}{\partial z}\right\}+\frac{\partial p}{\partial r} \quad =0, \tag{17}$$

$$\rho\left\{\frac{\partial w}{\partial t}+\frac{u\,\partial w}{\partial r}+\frac{w\,\partial w}{\partial z}\right\}+\frac{\partial p}{\partial z} \quad =0, \tag{18}$$

$$\frac{p'}{\rho'}=c^2, \tag{19}$$

where z and r refer to axial and radial positions, respectively, and u is the velocity in the radial direction.

Linearizing by allowing each property to be replaced by its mean and fluctuating component and neglecting second-order terms, one obtains, after some simplification,

$$\frac{\mathrm{d}U}{\mathrm{d}r}=-U\left\{\frac{1}{r}+\frac{k_z\mathrm{d}M/\mathrm{d}r}{k-Mk_z}\right\}+\frac{iP}{\rho_0 c}\left\{\frac{k_z^2}{k-Mk_z}-(k-Mk_z)\right\}, \tag{20}$$

$$\frac{1}{\rho_0 c}\frac{\mathrm{d}P}{\mathrm{d}r}=-iU\{k-Mk_z\}, \tag{21}$$

$$W=\frac{k_z P}{\rho_0 c(k-Mk_z)}+i\frac{U\dfrac{\mathrm{d}M}{\mathrm{d}r}}{k-Mk_z}, \tag{22}$$

where $M=M(r)$: Mach number, $p'=P(r).\mathrm{e}^{i(\omega t-k_z z)}$, $w'=W(r).\mathrm{e}^{i(\omega t-k_z z)}$, $u'=U(r).\mathrm{e}^{i(\omega t-k_z z)}$, $k=\omega/c$.

Before the solution can proceed, the form of the mean velocity profile across the radius must be known.

For fully developed turbulent flows, Schlichting [25] has shown that the velocity profile (in the absence of superimposed sound) is of the form

$$M=M_0\left\{\frac{y}{a}\right\}^{1/N}, \tag{23}$$

where M_0 is the midstream Mach number, y is the distance from the wall of the pipe (for radius a), and N is an exponent dependent on Reynolds number.

For typical Reynolds numbers in the exhaust pipe, namely 10^5, N is approximately 7. Measurements in the exhaust system showed, as noted previously, that the average Mach number was 85% of its midstream value which corresponds to an exponent more nearly 8·5. Since it was found the solution of the equations was relatively insensitive to the value of N but depended rather on the value of the mean velocity, this discrepancy was not serious. The fact that the flow was probably pulsating and that the pipe walls were unlagged may account for the observed difference in the value of N.

If the relation between radial particle velocity and pressure is known at the wall of the tube (for example, the wall admittance), equations (20) and (21) can be simply solved by numerical integration commencing at the wall and proceeding stepwise towards the centre. Equation (22) follows immediately. The fourth-order Runge-Cutta method [28] was found to be satisfactory and no special difficulties were encountered in handling the complex quantities. An iterative procedure based on the method of steepest descent [29] was written to determine the eigenvalues, k_z. Clearly, a large number of values are possible, all of which reduce the radial velocity, U, to zero at the centre-line (considering only the symmetric cases) and those

of course correspond to the various higher-order modes. Only the 0,0 modes in both the positive and negative directions are included here.

To give some indication of the variation of the quantities P, U, W, in typical exhaust systems, their moduli are plotted in Figure 9 for two values of the frequency parameter, ka. The first, 0·81, corresponds to 980 Hz in a 4·8 in. diameter pipe (Figure 6) and the second, 0·2 corresponds to 365 Hz in a 3 in. diameter pipe (Figure 7). Both rigid walls and slightly yielding

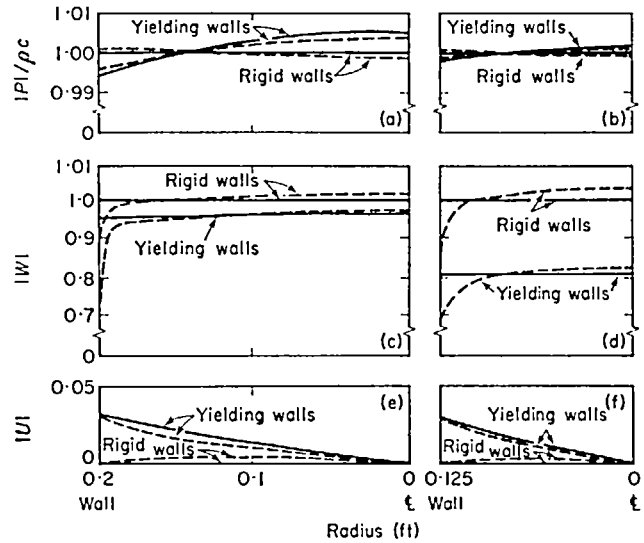

Figure 9. Radial variation of pressure and particle velocity. ——, Mean flow; – – – –, mean flow with shear. $|P|_{mean}/\rho_0 c = 1{\cdot}0$. For clarity only positive-going waves are shown.

(a) Modulus of pressure vs. radius at 980 Hz, $M = 0{\cdot}078$.
(b) Modulus of pressure vs. radius at 365 Hz, $M = 0.17$.
(c) Modulus of axial velocity vs. radius at 980 Hz, $M = 0{\cdot}078$.
(d) Modulus of axial velocity vs. radius at 365 Hz, $M = 0{\cdot}17$.
(e) Modulus of radial velocity vs. radius at 980 Hz, $M = 0.{\cdot}078$
(f) Modulus of radial velocity vs. radius at 365 Hz, $M = 0{\cdot}17$.

TABLE 1

Frequency (Hz)	Radius (ft)	Condition	Nett flux, $\rho_0 c/A^2$ Rigid walls	Yielding walls
980	0·20	Mean flow	0·645	0·620
		Mean flow + shear	0·644	0·609
		Mean flow + viscosity	0·645	—
365	0·125	Mean flow	0·628	0·525
		Mean flow + shear	0·623	0·430
		Mean flow + viscosity	0·628	—

The following assumptions are made:

(a) the modulus of the r.m.s. value of the incident pressure wave averaged over a cross-section = A;
(b) the modulus of the r.m.s. values of the reflected pressure wave averaged over a cross-section = $R.A$, where R is the reflection coefficient;
(c) for 980 Hz, $R = 0{\cdot}78$, $M = 0{\cdot}078$;
(d) for 365 Hz, $R = 1{\cdot}04$, $M = 0{\cdot}171$;
(e) normal wall admittance ratio for the yielding walls = $0{\cdot}0016 - i0{\cdot}032$.

walls are considered. For rigid walls, the admittance ratio is $0{\cdot}0 + i0{\cdot}0$. which of course corresponds to a reflection coefficient of unity and a phase angle of zero. For yielding walls the admittance ratio used was $0{\cdot}0016 - i0{\cdot}032$. This is a somewhat arbitrary selection but is used merely to gain some appreciation of the order of magnitude effect of yielding walls on the pressure and particle velocity profiles. The value of wall admittance ratio corresponds to a reflection coefficient of 0·998 and a phase angle between the reflected and incident waves of 0·02 radians. These values were considered typical of slightly yielding walls, but as indicated above the general conclusions do not depend critically on the exact value of this admittance ratio. The nett energy flux for both frequencies considered above is given in Table 1.

7.2. CASE (b) MEAN FLOW, ZERO SHEAR, YIELDING WALLS, INVISCID

To appreciate the effects of shear on nett energy transport, equations (16), (17) and (18) can be solved again with the mean velocity profile set constant at its average value. Under these conditions an exact solution is possible which substantially reduces the time taken to calculate the energy flux.

In the absence of shear, the equations combine to give

$$\frac{\mathrm{d}^2 P}{\mathrm{d}r^2} + \frac{1}{r}\frac{\mathrm{d}P}{\mathrm{d}r} + k^2\{(1 - MK)^2 - K^2\} = 0, \tag{24}$$

where $K = k_z/k$.

This is now a standard Bessel function equation which has the solution [26]

$$P = B.J_0(k_r r), \tag{25}$$

where B is a constant and k_r, generally complex, is given by

$$k_r^2 = k^2\{(1 - MK)^2 - K^2\}, \tag{26}$$

and J_0 is the Bessel function of the first kind of order zero.

Knowing the wall admittance ratio, β, and assuming only slightly yielding walls one can obtain (Appendix)

$$k_r^2 \simeq \frac{2ik\beta}{a}\{1 - MK^2\}, \tag{27}$$

where a is the pipe radius.

This equation can now be solved simultaneously with (26) to give both k_r and k_z. The radial variation in pressure follows immediately from (25), while the axial and radial particle velocities can be calculated from (22) and (21), respectively. The term involving $\mathrm{d}M/\mathrm{d}r$ in (22) is of course set equal to zero. The moduli of P, U and W are shown in Figure 9 for the two frequencies considered in case (a). Both rigid walls and yielding walls are considered. The corresponding nett energy flux is given in Table 1.

7.3. CASE (c) MEAN FLOW AND VISCOSITY, ZERO SHEAR, RIGID WALLS

The solution of the equations including viscous effects is very difficult due to the presence of higher-order terms and the complicated relationship between fluctuating pressure and density [27]. However, a rough order of magnitude estimate on the effect of energy flux in an exhaust system can be obtained by restricting the analysis to rigid walls (in which case the radial velocity U is approximately zero and the pressure P is approximately constant) and by assuming the pressure–density relationship of (19).

The linearized momentum equation now takes the form

$$\rho_0 \cdot \frac{D_0 w'}{Dt} + \frac{\partial p'}{\partial z} = \mu_0 \left\{ \frac{\partial^2 w'}{\partial r^2} + \frac{1}{r} \cdot \frac{\partial w'}{\partial r} + \frac{\partial^2 w'}{\partial z^2} \right\}, \tag{28}$$

where μ_0 is the coefficient of viscosity (and terms in μ' have been neglected) and

$$\frac{D_0}{Dt} = \frac{\partial}{\partial t} + w_0 \frac{\partial}{\partial z}.$$

This is an inhomogeneous Bessel equation which since fluctuating axial particle velocity is zero at the walls, has the solution,

$$W = \frac{-ik_z P}{\mu_0 D^2}\left\{1{\cdot}0 - \frac{J_0(D.r)}{J_0(D.a)}\right\}, \tag{29}$$

where

$$D^2 = \frac{-i\rho_0 c}{\mu_0}(k - Mk_z) - k_z^2. \tag{30}$$

Assuming now that in the presence of viscosity the relationship (19) is still nearly correct, one can relate the fluctuating axial velocity averaged over a cross-section to the mean pressure via the continuity equation, namely,

$$W_{av} \simeq \frac{P}{\rho_0 c}\frac{(k - Mk_z)}{k_z}. \tag{31}$$

Averaging equation (29) over a cross-section and utilizing standard Bessel function relations [26] one obtains

$$W_{av} = \frac{-ik_z P}{\mu_0 D^2}\left\{1{\cdot}0 + \frac{2i}{D.a}\right\}, \tag{32}$$

which can now be solved with (31) to give the axial wave number k_z and the parameter, D. The variation in fluctuating axial particle velocity follows immediately from (29).

It was found that the fluctuating axial particle velocity was virtually constant over the entire cross-section except for a very small region adjacent the tube walls. In this region (typically less than $\frac{1}{16}$ in.), the velocity decreased very rapidly from its maximum value to zero at the tube walls. Thus, knowing the variation in axial particle velocity (29), it is now possible to calculate the nett energy flux from (15). This is given in Table 1 for the two frequencies considered previously.

It can be seen that for rigid-walled tubes, the effect of shear and viscosity on nett energy flux is small for both frequencies and can for practical purposes be ignored in exhaust systems. When the walls yield, however, the influence is not necessarily small but dependent on (a) the magnitude of the radial velocity at the wall; (b) the Mach number of the flow; and (c) the frequency parameter, ka.

The particular property most affected is the axial velocity, W. Its average value is dependent primarily on the amount of yielding of the walls and the variations about this average value are a function mostly of the mean gas flow profile.

The variation in pressure across the radius is very slight. It increases as the frequency parameter ka increases and as the yielding of the wall increases. For practical purposes in exhaust systems, this variation can be neglected. The reductions in nett energy flux due to the simultaneous effects of shear and yielding walls for the two frequencies given above are approximately –0·5 dB(980 Hz) and –3·2 dB(365 Hz).

7.4. YIELDING OF WALLS IN EXHAUST SYSTEM

Before an assessment of the reduction in nett energy flux due to shear, and yielding walls can be made for the standing waves of section 6, there must be some appreciation of the amount of yielding of the walls of the tubes. This can be obtained by observing the rise in the

minima of the standing waves of Figures 6 and 7. The ratio of two minima $|p_1|$ and $|p_2|$ at axial positions z_1 and z_2 is given, from (8) and (9), by

$$\frac{|p_1|}{|p_2|} = \frac{|1 - R.e^{(k_4 - k_2)z_1}|}{|1 - R.e^{(k_4 - k_2)z_2}|}, \tag{33}$$

$$\doteq \frac{1 - R + z_1(k_2 - Rk_4)}{1 - R + z_2(k_2 - Rk_4)}. \tag{34}$$

On the basis of the analysis of case (a) and case (b),

$$k_4 \doteq -1{\cdot}5\, k_2 \text{ for } M = 0{\cdot}171,$$

which allows an approximation to the imaginary parts (k_2, k_4) of the wave numbers. These were found to be typically only of the order of one-third of those calculated for the assumed wall admittance ratio of $0{\cdot}0016 - i0{\cdot}032$. Consequently, the amount of yielding of the walls that is actually occurring is less than that initially assumed. The reduction in nett flux due to shear and yielding compared with the rigid wall zero shear case is therefore probably only about 1 dB. Under these circumstances, it is simplest to assume that the mean flow velocity

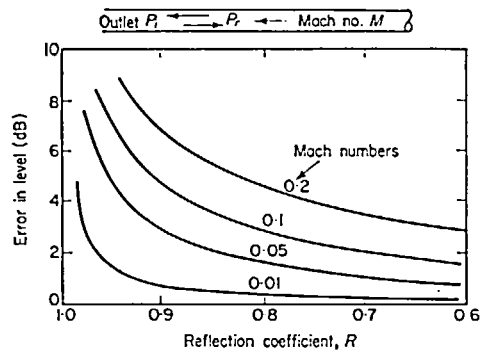

Figure 10. Radiated sound pressure level error due to neglect of mean flow. $P_r = R.Pe^{i\theta}$. Radiated sound pressure level calculated neglecting mean flow is low by the amount given here as error,

$$\text{Error} = 10 \log \left[\frac{(1 + M)^2 - R^2(1 - M)^2}{1 - R^2} \right].$$

profile is invariant, and to make a subsequent reduction to the nett energy flux. With this procedure, equation (15) now reduces to

$$I = \frac{A^2_{\text{r.m.s.}}}{\rho_0 c} \{(1 + M)^2 - R^2(1 - M)^2\}, \tag{35}$$

where $A_{\text{r.m.s.}}$ is the root mean square amplitude of the incident pressure wave at the exhaust outlet, and R is the reflection coefficient.

It is interesting to compare the flux of (35) with that for zero mean gas flow, namely,

$$I = \frac{A^2_{\text{r.m.s.}}}{\rho_0 c} (1 - R^2). \tag{36}$$

The effect of mean flow, therefore, on nett energy flux in an exhaust system becomes important in the region of R approximately equal to unity. Under these conditions, equation (36) approaches zero while (35) remains finite. The resulting error in nett flux from the neglect of mean flow is therefore very large, even when the Mach number of the flow is small, as is shown in Figure 10. The fact demonstrates also that the use of normal electrical analogue

simulation of the exhaust system or the solution of the acoustic equations neglecting flow is significantly in error in the region of most interest, that is at the lower frequencies.

Note from (35) that the value of the reflection coefficient can exceed unity. The maximum value before flux reversal occurs is now given by

$$R_{\max} = \frac{1+M}{1-M}.$$

8. CALCULATION OF THE LEVEL OF THE RADIATED SOUND

The level of the sound radiated by the exhaust outlet can be obtained by equating the nett energy in the tail pipe to that of a spherically diverging wave. This gives

$$\pi a^2 \frac{A^2_{\text{r.m.s.}}}{\rho_0 c_0}\{(1+M)^2 - R^2(1-M)^2\} = 4\pi r^2 \frac{B^2_{\text{r.m.s.}}}{\rho_1 c_1}, \tag{37}$$

TABLE 2

Frequency (Hz)	Pipe radius (ft)	Mach no.	Calculated level (dB)	Measured level (dB)
228	0·20	0·078	112	112
275	0·20	0·078	113	111
342	0·20	0·078	116	115
545	0·20	0·078	98	98
685	0·20	0·078	91	93
796	0·20	0·078	97	96
980	0·20	0·078	100	98
365	0·125	0·171	108	106
485	0·125	0·171	99	97
610	0·125	0·171	101	100
830	0·125	0·171	94	93
965	0·125	0·171	94	93
1105	0·125	0·171	95	95
1325	0·125	0·171	93	94

where the subscripts 0 and 1 refer to conditions inside and outside the pipe, respectively. The quantity $B_{\text{r.m.s.}}$ is the root mean square amplitude of the spherical pressure wave at a radius r from the exhaust outlet. The remaining symbols have been defined previously.

Thus, knowing the quantities $A_{\text{r.m.s.}}$, ρ_0, c_0, R and M from measurements in the exhaust pipe and the quantities ρ_1 and c_1 from the temperature of the surrounding air, one can calculate the average level of the radiated sound.

Table 2 summarizes the calculated and measured levels of the radiated sound pressure levels for two of the several tests conducted. These correspond to the maximum and minimum Mach numbers. (Some of the standing waves are given in Figures 6 and 7.) The calculated levels assume rigid walls.

It can be seen that the calculated levels are sufficiently accurate for design purposes. Those at the lower Mach numbers agree better with the measured values than those at the higher Mach number. This is considered to be due to non-plane wave effects, which, as discussed earlier, become more important with higher Mach numbers and smaller pipe diameters. It is likely too that losses occur during the exiting process since it has been established [30] that ring vortices form at the exit and are shed in synchronism with the radiating frequencies.

Since this effect is apparently small in the present situation and is, in any case, beneficial so far as the level of the radiated sound is concerned, there has been no further investigation into this particular phenomenon.

9. CONCLUSIONS

The fluctuating pressures in the tail pipe of an exhaust system are small compared with the mean pressure. A linearized theory with mean flow can therefore describe the behaviour sufficiently accurately for design purposes.

It is possible to use the tail pipe as an impedance tube (with the engine exhaust system as the source of the signals) to measure the reflection coefficient and phase angle at the exhaust outlet.

The magnitude of the reflection coefficient at the exhaust outlet is greater than that predicted for the zero flow case. The phase angle is not greatly affected by the presence of the exhaust gas flow.

The nett energy flux in the tail pipe can be calculated by assuming plane mode propagation. The effect of shear on this flux is generally small unless there is some significant yielding of the walls of the tube.

The level of the radiated sound can be related to the nett energy flux. The neglect of mean flow will lead to a considerable underestimation of the level of the radiated sound.

ACKNOWLEDGMENTS

We are appreciative of helpful discussion with our colleagues at the Institute of Sound and Vibration Research and of the assistance given by technical staff, particularly Mr F. Cummins, in performing the engine tests.

REFERENCES

1. B. G. WATTERS, R. M. HOOVER and P. A. FRANKEN 1959 *Noise Control* **5**, 18. Designing a muffler for small engines.
2. D. DAVIES, G. W. STOKES, D. MOORE and G. L. STEVENS 1954 *NACA Rep. 1192* Theoretical and experimental investigation of mufflers with comments on engine exhaust muffler design.
3. Y. N. CHEN 1967–68 *Proc. Instn Mech. Engnrs* **182**, 60. Lateral Helmholtz resonator silencer with turbulence absorption.
4. V. O. RATHFUB 1959 *Techn. Mitt. Krupp* **17**, 172. Das Auspuffgerausch und Dampfung bei lastkraftwagen mit 2 Takt-Motoren.
5. R. KAMO 1959 *Am. Soc. mech. Engnrs preprint 58-A-144.* Suppression of engine exhaust noise.
6. T. A. DANNER 1959 *Soc. automot. Engnrs preprint 38T.* Muffler location is important.
7. L. E. MULLER 1959 *Soc. automot. Engnrs preprint 38R.* Exhaust systems, fundamentals and design considerations.
8. M. H. NASSIF 1969 *J. mech. Engng. Sci.* **11**,402. Acoustical analysis applied to internal combustion engine exhaust systems of conical form.
9. P. O. A. L. DAVIES 1964 *J. Sound Vib.* **1**, 185. The design of silencers for internal combustion engines.
10. C. RUDINGER 1955 *Wave Diagrams for Non Steady Flow in Ducts* New York: D. Van Nostrand Co.
11. R. S. BENSON and K. GALLOWAY 1968–69 *Proc. Instn mech. Engnrs* **183**, 253. An experimental and analytical investigation of the gas exchange process in a multi-cylinder pressure charged two stroke engine.
12. R. S. BENSON 1967–68 *Proc. Instn mech. Engnrs* **182**, 95. A programme for calculating the performance of an internal combustion engine exhaust system.
13. L. E. KINSLER and A. R. FREY 1966 *Fundamentals of Acoustics* pp. 217–246. New York: John Wiley & Sons.

14. H. LEVINE and J. SCHWINGER 1948 *J. Phys. Rev.* **73**, 383, On the radiation of sound from an unflanged circular pipe.
15. C. H. G. MILLS and P. W. ROBINSON 1961 *Engineer, Lond.* (June) p. 1070. The subjective rating of motor vehicle noise.
16. R. R. HILLQUIST 1967 *Sound Vib.* (April) p. 8. Objective and subjective measurement of truck noise.
17. V. MASON 1969 *J. Sound Vib.* **10**, 2, 208. Some experiments on the propagation of sound along a cylindrical duct containing flowing air.
18. F. P. MECHEL, P. A. MERTENS and W. M. SCHILZ 1967 *AMRL-TR-67-120 (II)*. Interaction between air flow and airborne sound in a duct.
19. L. L. BERANEK 1940 *J. acoust. Soc. Am.* **12**, 3. Precision measurement of acoustic impedance.
20. 1958 *A.S.T.M. C 384-58* p. 134. Standard method of test for impedance and absorption of acoustical materials by the tube method.
21. F. MECHEL, W. SCHILZ and J. DIETZ 1965 *Acustica* **15**, 199. Akustische Impedanz einer Luft-durchstromten Offnung.
22. C. M. HARRIS (Ed.) 1957 *Handbook of Noise Control* p. 17.28. New York: McGraw-Hill.
23. C. L. MORFEY 1967 *Bolt, Beranek & Newman Rep. 1547*. Energy balance equations in acoustics.
24. S. PAI 1956 *Viscous Flow Theory* part I, p. 38. New York: D. Van Nostrand Co.
25. H. SCHLICHTING 1955 *Boundary Layer Theory* p. 504. New York: McGraw-Hill.
26. JAHNKE-EMDE-LORCH 1966 *Tables of Higher Functions* 7th Edition, p. 156. Stuttgart: B.G. Teubner Verlagsgesellschaft.
27. P. MUNGUR and G. M. L. GLADWELL 1969 *J. Sound Vib.* **9**, 28. Acoustic wave propagation in a sheared fluid contained in a duct.
28. R. S. KUNZ 1957 *Numerical Analysis* p. 188. New York: McGraw-Hill.
29. G. A. KORN and T. H. KORN 1961 *Mathematical Handbook for Scientists and Engineers* p. 634. New York: McGraw-Hill.
30. U. INGARD and S. LABATE 1950 *J. acoust. Soc. Am.* **22**, 211. Acoustic circulation effects and the non-linear impedance of orifices.

APPENDIX

RELATION BETWEEN WALL ADMITTANCE AND RADIAL WAVE NUMBER

Due to the relative motion between the mean flow and the wall of the pipe, the ratio of the radial velocity to the fluctuating pressure at the wall is no longer simply related by the wall admittance but takes rather the form [27]

$$\beta = \frac{i\dfrac{\mathrm{d}P}{\mathrm{d}r}}{Pk(1-MK)^2}, \tag{A1}$$

where β is the wall admittance ratio and K is the normalized axial wave number, (k_z/k).

The pressure, P, and the pressure gradient in the radial direction, $\mathrm{d}P/\mathrm{d}r$, are evaluated at the wall, i.e. $r = a$.

Substituting (25) reduces the above equation to

$$\beta = -i\frac{kr}{k}\frac{J_1(k_r a)}{J_0(k_r a)}\cdot\frac{1}{(1-MK)^2}, \tag{A2}$$

where J_1 is the Bessel function of the first kind of order unity.

If one is now concerned with the 0,0 mode and only slightly yielding walls, the Bessel functions J_1 and J_0 can be approximated by

$$J_0(k_r a) = 1{\cdot}0 - (k_r a)^2/2, \tag{A3}$$

$$J_1(k_r a) = k_r a/2. \tag{A4}$$

Substitution of these equations into (A2) produces

$$k_r^2 \simeq \frac{2ik\beta}{a}\{1-MK\}^2.$$